Nonlinear Dyn (2021) 104:971–988
https://doi.org/10.1007/s11071-021-06369-4

ORIGINAL PAPER

Stochastic resonance in cascaded monostable systems with double feedback and its application in rolling bearing fault feature extraction

Jimeng Li · Xiangdong Wang · Zhixin Li · Yungang Zhang

Received: 22 October 2019 / Accepted: 12 March 2021 / Published online: 17 March 2021

Abstract Stochastic resonance (SR) has been widely concerned and studied in the field of mechanical fault detection due to the capability of weak signal detection. However, research focused on how to improve the performance of SR system and enable it to process large-parameter signals in engineering practice better. Therefore, from the perspective of feedback control and multi-system synergy, this paper presents a double-feedback cascaded monostable SR (CMSR) system and analyzes the SR phenomenon in the system by using the signal-to-noise ratio as the measurement index. It investigates specifically influence of the coefficients on the system performance. Introducing feedback control and serial structure to a monostable system, consisting of a symmetric quartic potential function, not only alters the response characteristics of the monostable system but also significantly improve the system performance. Compared with the classical bistable SR system with low-pass filtering characteristics, the proposed system can exhibit low-pass filtering or band-pass filtering behavior through different combinations of feedback coefficients, which can better match the frequency characteristic of target signal. Finally, the proposed double-feedback CMSR system is used for extraction of the weak signal features in rolling bearing fault detection, and its superiority and feasibility are verified by comparison with other SR systems.

Keywords Stochastic resonance · Double feedback · Cascaded monostable system · Weak signal detection · Fault feature extraction

1 Introduction

Vibration analysis has been widely used in the condition monitoring and fault diagnosis of rotating machinery [1–4] and plays an important role in equipment maintenance. Vibration signals, as an important carrier of the operating status information of mechanical equipment, are the basic media for people to understand and master the health status of mechanical equipment. However, some influential factors such as the complex structure of equipment, various vibration transmission paths, and strong background noise interferences weaken the useful information contained in the collected vibration signals, which in turn increases the difficulty of identifying the health status of the equipment. Therefore, it is of great importance to accurately identify the useful information in vibration signals to detect the existing faults as early as possible and to ensure the safe and reliable operation of the equipment through timely maintenance. Accordingly, scholars have

J. Li (✉) · X. Wang · Z. Li · Y. Zhang
College of Electrical Engineering, Yanshan University, Qinhuangdao 066004, People's Republic of China
e-mail: xjtuljm@163.com

investigated and developed many effective signal processing techniques for fault diagnosis of rotating machinery, for example, nonlinear mode decomposition [5], variational mode decomposition [6], intrinsic time-scale decomposition [7], empirical mode decomposition [8], time–frequency analysis [9, 10], etc. These methods have been successfully applied in fault diagnosis of gears, bearings, etc., but they almost all highlight the target signal by suppressing or filtering out noise. Therefore, the useful features are also inevitably weakened while denoising the signals, especially when the noise interferences are the same as the frequency of the target signal. Different from the above methods, stochastic resonance (SR), as a nonlinear signal processing method, regards noise as energy and can enhance weak signals by utilizing noise with the help of nonlinear systems. This is providing a powerful tool for weak signal detection.

SR was first proposed by Benzi et al. to explain the periodicity of the Earth's ice climate [11]. Initially, within the constraint of the adiabatic approximation theory, SR can only process small-parameter signals (i.e., the signal frequency is much smaller than 1 Hz). To break through this limitation, scholars have carried out lots of research to enable SR to process large-parameter signals (i.e., the signal frequency is much larger than 1 Hz) in engineering practice, and have made fruitful achievements, thus promoting the development of SR theory and its application in the field of mechanical fault diagnosis [12–16]. For example, He et al. [13] used SR to analyze vibration signals of the automobile gearbox and diagnosed the wear failure of the gear accurately. Li et al. [17] adopted SR to analyze vibration signals of gearbox of a rolling mill, and the fault of rolling bearing was successfully detected. He et al. [18] applied SR to diagnose the blade crack of compressor and achieved good results. From the stochastic dynamics and Brownian motion, the potential function models, as an important component of SR system, have an important influence on the system output determined by the motion trajectory of Brownian particles in the potential function. In order to improve the performance of SR for weak signal detection, various SR methods based on different potential models have been investigated in the past few decades. The SR methods based on the bistable model are firstly concerned and studied by scholars. It not only has gained abundant results in theory, but also has solved many practical problems [19, 20]. In a bistable system excited by the combination of a weak low-frequency signal and noise, Yang et al. [21] used numerical methods to analyze the noise-induced resonance at the subharmonic frequency which equals to 1/3 multiple of the driving frequency, indicating that in addition to the resonance at the driving frequency, the resonance at the subharmonic frequency should never be neglected. To solve the output saturation problem of the classical bistable SR (CBSR) system, Qiao et al. [22] constructed a piecewise unsaturated bistable SR system by changing the shape of the bistable potential function, and successfully diagnosed the planetary gearbox faults. Based on the overdamped and underdamped bistable SR system, Liu et al. [23] realized the vibration resonance detection of weak high-frequency character signals, which makes it possible to deal with the engineering problems using the theory of vibration theory. In addition to the bistable potential models, SR phenomena based on monostable and multi-stable potential functions have also been extensively studied to accommodate the variety of requirements [24]. For example, Agudov et al. [25] studied SR phenomenon in a trapping overdamped system with a piecewise linear monostable potential function and analyzed the system dynamic characteristics. Yao et al. [26] studied SR phenomenon in a bias monostable SR (MSR) system driven by a periodic rectangular signal and uncorrelated noise, and the analysis results indicated that the bias parameter had an important influence on the system output SNR. Han et al. [27] proposed a multi-stable SR system based on parameter compensation to effectively increase the amplitude of system response. Aiming at the problem of non-standardized tristable potential functions, Lai et al. [28] proposed a standard tristable SR system based on a symmetric tristable potential function and analyzed multi-parameter adjustment strategy and its applications. Lei et al. [29] proposed an underdamped multi-stable SR system that behaved like a band-pass filter and was capable of suppressing the multi-scale noise. These research results have effectively promoted the development of SR and improved the performance of SR system.

In addition, some research results demonstrate that the detection performance of SR system for weak signals can also be improved by introducing time-delayed and feedback parameters [30, 31]. For example, Hu et al. [32] studied the influence of multiple

time-delayed feedback parameters on the bistable SR system, and the proposed multi-time-delayed feedback SR can make the signal output waveform smoother and improve the system output SNR. Lu et al. [33] introduced the time-delayed feedback parameters into the CBSR system, so that the system exhibited band-pass filtering behavior. The introduction of time-delayed feedback parameters can indirectly change the shape of the potential function, thereby affecting the system output performance. Furthermore, compared to the SR in a single system, the SR system based on multi-system synergy can comprehensively utilize the effective information of each subsystem and has more advantages in weak signal detection. The cascaded bistable SR system can make the system output smoother and increase the output SNR by connecting multiple subsystems in series [34–36]. By studying SR phenomenon in parallel array of bistable systems, it is found that the nonlinear collective characteristic of parallel arrays can further improve the system output SNR gain and enhance the system's robustness [38, 39]. The coupled SR system can enrich the response characteristics of the system by utilizing the coupling effect between multiple systems, thereby obtaining better performance of SR system [39–41]. The results indicated that the response characteristics of a single system can be changed by the coupling effect between multiple systems to obtain better system performance.

The above research results indicate that the performance of SR system can be improved by feedback control or the synergy of multiple systems, but in the current study, only the influence of a single factor is considered, and the two have not yet been organically combined with SR system. Therefore, it is necessary to study SR phenomenon under the common effect of feedback control and multi-system synergy to provide basis for the performance improvement and practical application of SR system. Therefore, by introducing feedback control and serial structure, this paper proposes a double-feedback cascaded monostable SR (CMSR) system based on a symmetric quartic monostable potential function and analyzes the SR phenomenon in the system driven by a periodic signal and Gaussian white noise. The proposed SR system consists of two monostable systems connected in series, and the system output is added to the inputs of the two subsystems by using feedback coefficients, thereby improving the overall performance of the system. The numerical analysis results indicate that compared with the monostable system, the proposed double-feedback cascaded monostable system can not only generate SR, but also has band-pass filtering characteristics, and its performance is superior to the CBSR system and the underdamped bistable SR (UBSR) system. Finally, the proposed SR system is used to extract the weak signal features and realize the fault detection of rolling bearings.

The rest of this paper is arranged as follows. Section 2 introduces the double-feedback CMSR system and analyzes in detail the influence of system parameters on the performance. In Sect. 3, by comparing with other SR systems, numerical simulation is carried out to analyze the performance of the proposed system. In Sect. 4, the proposed SR system is applied to detect the weak signals, and two sets of rolling bearing fault feature extraction examples are provided. Some conclusions are presented in Sect. 5.

2 Double-feedback CMSR system

2.1 Mathematical model

According to the automatic control theory, the feedback control is to input part or all of the system output back to the input terminal, thereby controlling the system output and improving system performance. Cascaded SR system is composed of multiple single SR systems connected in series. In cascaded SR system, the output of the former stage system is used as the input of the latter system, and through the repeated processing of multi-level systems for the input signal, the noise can be further weakened, thereby realizing the enhanced extraction of the weak signal features. Based on the classical SR theory, by introducing feedback control parameters, the double-feedback CMSR system constructed in this paper is described as follows:

$$\begin{cases} \dfrac{\mathrm{d}x_1(t)}{dt} = -\dfrac{\partial U_1(x_1,t)}{\partial x_1} + s(t) + \xi(t) + k_1 x_2(t) \\ \dfrac{\mathrm{d}x_2(t)}{dt} = -\dfrac{\partial U_2(x_2,t)}{\partial x_2} + x_1(t) + k_2 x_2(t) \end{cases} \tag{1}$$

where $s(t)$ is the periodic input signal, $\xi(t)$ is a Gaussian white noise with intensity D and mean zero,

$x_1(t)$ is the output of the first-stage subsystem and the input of the second-stage subsystem, $x_2(t)$ is the output of the second-stage subsystem and also the final output of the cascaded system. Moreover, by introducing feedback parameters k_1 and k_2, the output $x_2(t)$ is introduced to the inputs of the first-stage subsystem and the second-stage subsystem, respectively, to improve the dynamic response performance of the cascaded system. $U_i(x_i, t)$ is a symmetric quartic monostable potential function, described as follows:

$$U_i(x_i, t) = \frac{a_i}{4} x_i^4(t) \quad i = 1, 2 \tag{2}$$

where a_i is the model parameter, which is a real number greater than zero. The schematic diagram of the system structure obtained according to Eq. (1) is illustrated in Fig. 1a. For comparison, the schematic diagrams of feedback monostable SR (MSR) system and CBSR system are provided in Fig. 1b, c.

In this paper, in order to analyze the dynamic response performance of the double-feedback CMSR system, the numerical method based on the fourth-order Runge–Kutta (RK4) equation is utilized to calculate the numerical solution of the system output [13].

As a widely used measurement index, the SNR can quantitatively describe the periodic components in a signal. Therefore, the SNR is used to evaluate the detection performance of the proposed system for weak signals. The SNR calculation formula used in this paper is as follows [19]:

$$\mathrm{SNR} = 10 \log_{10}\left(\frac{S(f_0)}{N(f) - S(f_0)}\right) \tag{3}$$

where f_0 denotes the target signal frequency, $S(f_0)$ is the amplitude corresponding to the target signal frequency in the spectrum, and $N(f)$ denotes the sum of the all amplitudes in the spectrum.

Next, two sets of numerical simulations are conducted to analyze the changing trends of the output SNR of the proposed double-feedback CMSR system with the noise intensity and make comparison with the feedback monostable SR (MSR) system, the CBSR system and the monostable system. In the first experiment, the periodic input signal is $s(t) = 0.1\sin(2\pi f_0 t)$, and the signal frequency is $f_0 = 0.01$ Hz, the sampling frequency is $f_s = 5$ Hz, and the data length is $N = 5000$ data points. The parameters of the double-feedback CMSR system are $a_1 = a_2 = 1.2$ and $k_1 = k_2 = 0.2$; the parameters of the feedback MSR system are $a = 1.2$ and $k = 0.2$; the parameters of the CBSR system are $a = b = 1.2$, and the parameter of the monostable system is $a = 1.2$. Adding Gaussian white noise to the system, the change range of noise intensity is [0.25 2.5], and the obtained system output SNR curves are shown in Fig. 2a, in which every curve is obtained by averaging 200 independent realizations. It can be found that the output SNRs of three systems including the proposed system, the feedback MSR system and the CBSR system firstly increase and then decrease with the increase of noise intensity, which indicates that there is a suitable noise intensity to make the system output SNR reach the maximum value, indicating the occurrence of SR phenomenon. Moreover, for the same noise intensity, the output SNR of the proposed system is significantly larger than the other two systems, indicating that the proposed system has better extraction capability for periodic signals. In addition, the output SNR of the monostable system monotonically decreases with increasing noise intensity, which

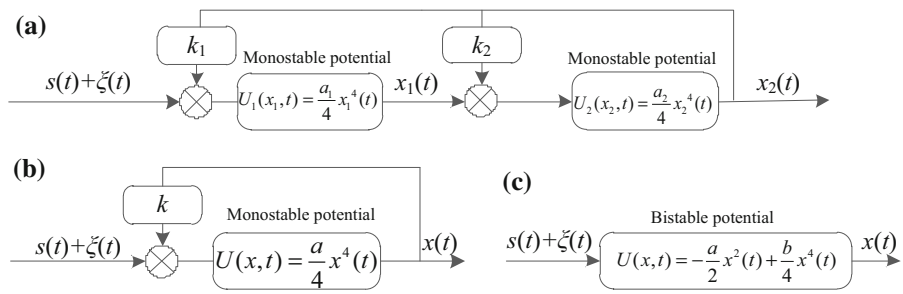

Fig. 1 The schematic diagrams of SR systems: **a** double-feedback CMSR; **b** feedback MSR; **c** CBSR

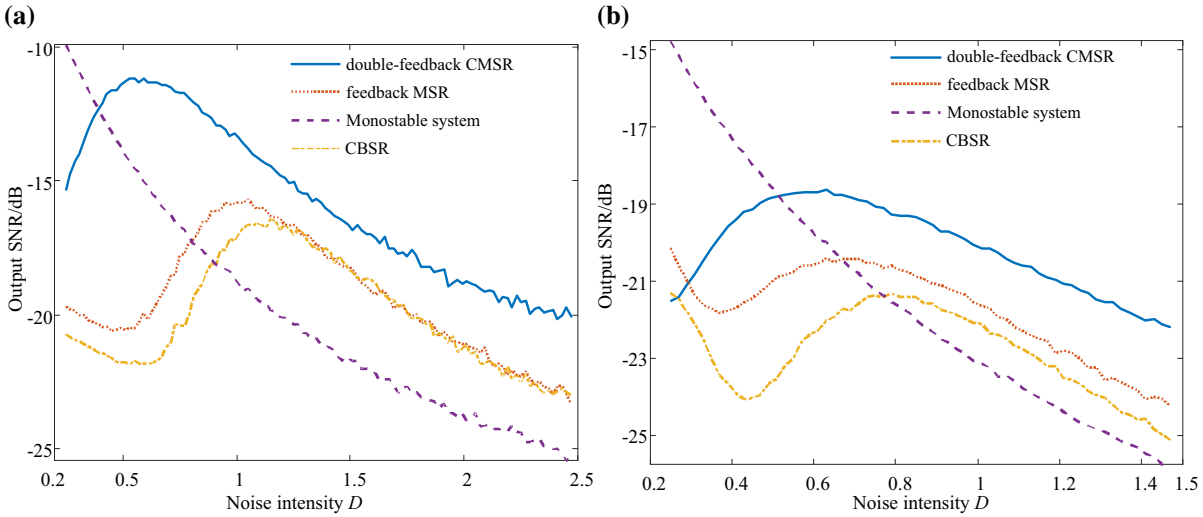

Fig. 2 System output SNRs versus noise intensity: **a** small-parameter input signal; **b** large-parameter input signal

indicates that the monostable system fails to generate resonance phenomenon. Therefore, comparing the proposed system, the monostable system and the feedback MSR system, it can be found that by introducing output feedback in the monostable system, the dynamic response characteristics of the system can be improved. From the perspective of the model, in the monostable system, feeding back the output to the input is equivalent to indirectly converting the monostable potential into a bistable potential, so that adding feedback to the monostable system, will provide a similar response to the bistable system. This can be verified by the output SNR curves of the feedback MSR system and the CBSR system, and the subsequent numerical simulation results.

In the second experiment, the large-parameter signal is used to analyze the changing trends of the system output SNR with the noise intensity. The large-parameter periodic input signal is $s(t) = 0.1\sin(2\pi f_0 t)$, the frequency is $f_0 = 120$ Hz, the sampling frequency is $f_s = 10$ kHz, the data length is $N = 10{,}000$, and the re-scaling ratio is $R = 3600$. The parameters of the system proposed in this paper are $a_1 = 1.2$, $a_2 = 2$, $k_1 = k_2 = 0.25$; the parameters of the feedback MSR system are $a = 1.2$ and $k = 0.25$; the parameters of the CBSR system are $a = 1.2$ and $b = 2$; the parameter of the monostable system is $a = 1.2$. The change range of noise intensity is [0.25 1.5], and the average SNR curves obtained by 200 independent realizations are shown in Fig. 2b. It is observed that for the large-parameter input signal, the system proposed in this paper, the feedback MSR system and the CBSR system can generate SR phenomenon, and for the same noise intensity, the output SNR of the proposed system is greater than the other two systems. This demonstrates that the system proposed in this paper has certain advantages for the detection of large-parameter signals and can be used for weak signal detection in engineering practice. Similarly, for the large-parameter signal, the monostable system still fails to generate resonance phenomenon. The above analysis indicates that the overdamped monostable system based on the symmetric quartic potential function cannot produce SR. However, by applying output feedback to it, the dynamic response characteristics of overdamped monostable system can be improved, making it capable of enhancing the weak input signals.

2.2 Performance analysis

a. Influence of system parameters on the output SNR
According to the theory of parameter-tuning SR, in addition to adjusting noise intensity, system parameters are also important factors in controlling the output of SR system. Accordingly, two sets of numerical simulations are carried out to analyze the influence of system parameters on the output SNR of the proposed system. In the first experiment, the input signal is $s(t) = 0.2\sin(2\pi f_0 t) + n(t)$, and the frequency is $f_0 = 0.1$ Hz, $\xi(t)$ is

Gaussian white noise with intensity $D = 1$. The sampling frequency is $f_s = 5$ Hz and the data length is $N = 4000$. Under the premise that other parameters of the proposed system are constant, the changing trend of system output SNR versus one parameter is analyzed, and the results obtained by calculating the average of 100 trials are shown in Fig. 3. It is observed that with the change of a single parameter, the system output SNR shows a trend of increasing first and then decreasing, indicating the occurrence of SR phenomenon. However, the change of the output SNR curves in Fig. 3b is more dramatic than that in Fig. 3a, which indicates that the system output is more sensitive to the feedback coefficients compared with the model parameters a_1 and a_2, further validating the important role of feedback control to the proposed system. Similarly, in Fig. 3b, the effect of feedback coefficient k_1 on the system output is more obvious than that of parameter k_2. Therefore, by adjusting system parameters, the proposed system can generate resonance phenomenon, and there is an optimal combination of parameters to maximize the system output SNR, thus realizing the detection of weak periodic signals.

In order to further reveal the influence of system parameters on the system output SNR, the changing trends of the system output SNR with noise intensity under different parameters are analyzed. In the experiments, the input signal is $s(t) = 0.1\sin(2\pi f_0 t) + n(t)$, and the frequency is $f_0 = 0.01$ Hz, the sampling frequency is $f_s = 5$ Hz, the data length is $N = 5000$. $\xi(t)$ is a Gaussian white noise with mean zero, and its intensity ranges from 0.25 to 2. First, in the case where the parameters a_2, k_1 and k_2 are constant, Fig. 4a displays the changing trends of the system output SNR versus noise intensity under different parameter a_1. It can be found that with the gradual increase of the parameter a_1, the optimal value of the system output SNR is gradually increasing, but the noise intensity corresponding to the optimal SNR is gradually decreasing. Similarly, the influence of parameter a_2 on the system output SNR is the same as that of parameter a_1. This shows that when the SNR of the input signal is low, the smaller parameters a_1 and a_2 are beneficial to the resonance detection of the periodic signal, contrariwise the larger parameters should be selected.

Next, under the premise of the constant parameters a_1, a_2 and k_2, the influence of the feedback coefficient k_1 on the system output SNR is analyzed, and the obtained results are shown in Fig. 4c. It is observed that with the increase of parameter k_1, the optimal value of the output SNR gradually decreases, but the noise intensity corresponding to the optimal SNR gradually increases. Comparing Fig. 4c with Fig. 4d, it can be found that the parameters k_2 and k_1 have similar effects

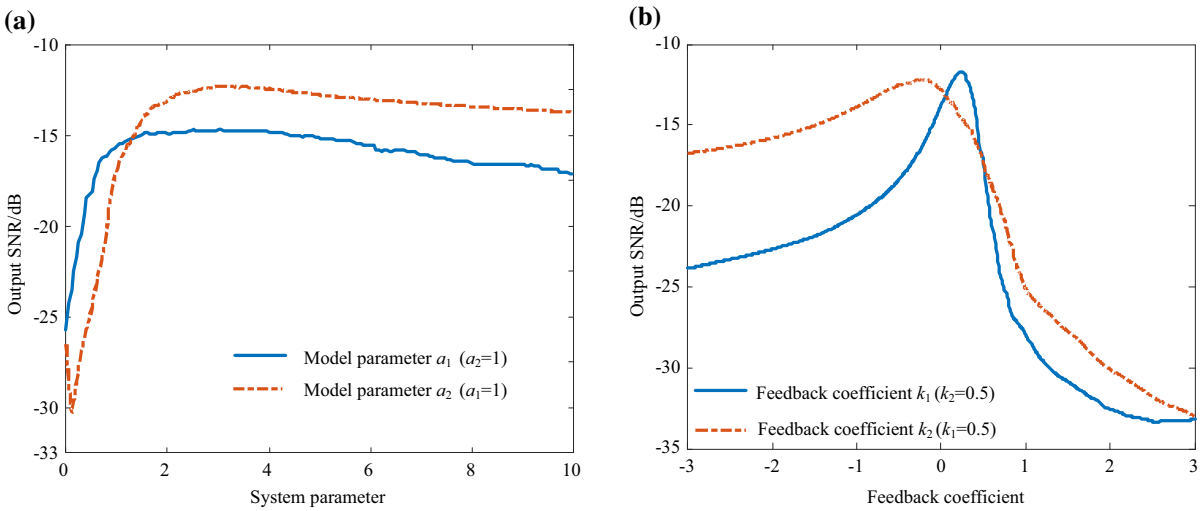

Fig. 3 Changing trends of system output SNR versus system parameters: **a** different model parameters ($k_1 = k_2 = 0.5$); **b** different feedback coefficients ($a_1 = a_2 = 1$)

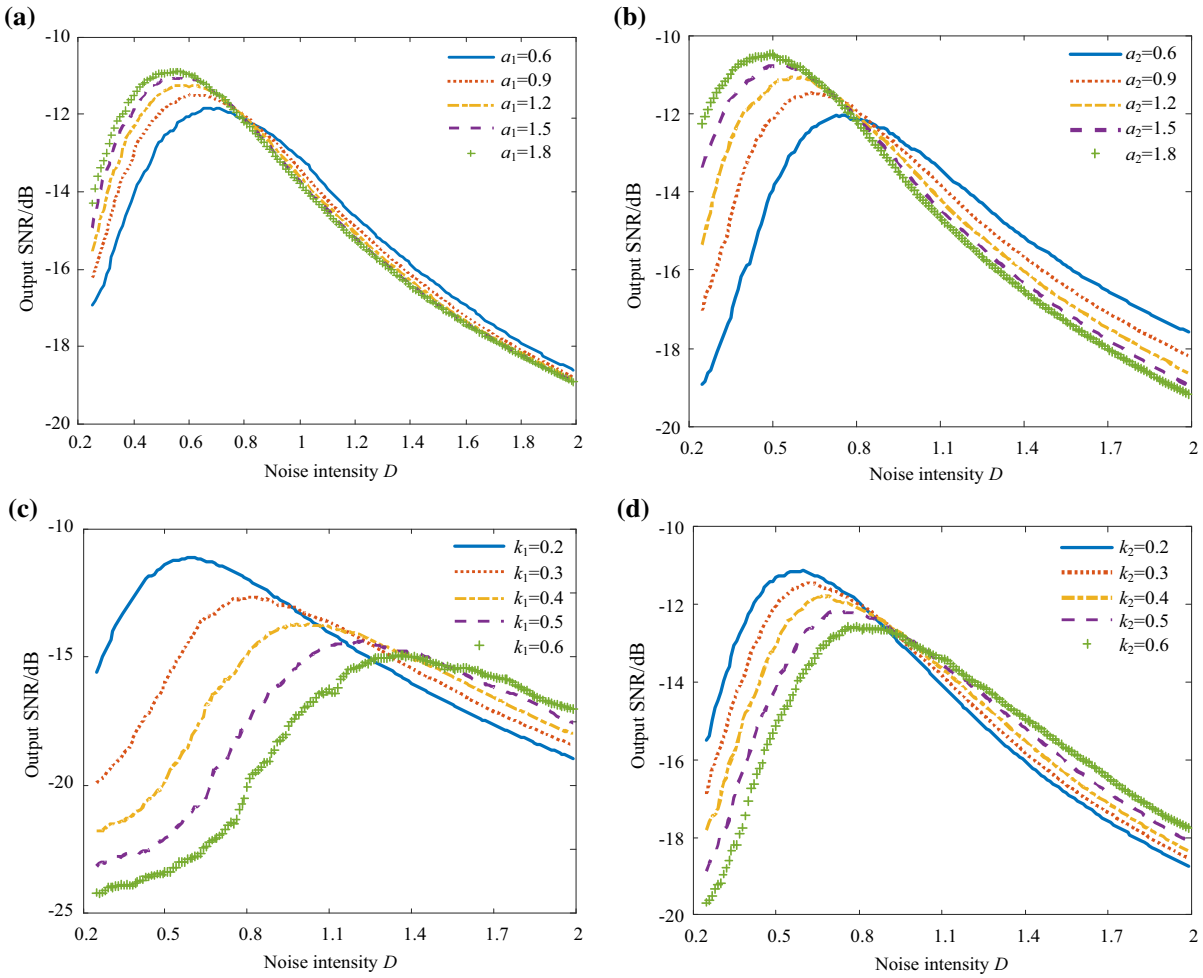

Fig. 4 Changes of system output SNR versus noise intensity under different parameters: **a** $a_2 = 1.2$, $k_1 = k_2 = 0.2$; **b** $a_1 = 1.2$, $k_1 = k_2 = 0.2$; **c** $a_1 = a_2 = 1.2$, $k_2 = 0.2$; **d** $a_1 = a_2 = 1.2$, $k_1 = 0.2$

on the system output. This indicates that larger feedback coefficients are suitable for detecting low SNR input signals. Through the above analysis, when the proposed system is used to detect periodic input signals, the selection of parameters a_1 and a_2 has an approximately negative correlation with the noise intensity of input signal, and the selection of feedback coefficients k_1 and k_2 are approximately positively correlated with the noise intensity of input signal.

b. Frequency response of system output

According to the previous analysis, the dynamic response characteristics of the monostable system are changed by introducing feedback control. Next, the numerical simulation is conducted to further analyze the output frequency response of the proposed system, and the effect of feedback control on the system response is validated by comparison with the CBSR system and the feedback MSR system. In the experiments, the input signal is $s(t) = 0.2\sin(2\pi f_0 t) + n(t)$, and $\xi(t)$ is Gaussian white noise with intensity $D = 1$, the sampling frequency is $f_s = 5000$ Hz, the data length is $N = 10{,}000$. The frequency of the input signal ranges from 10 to 200 Hz, and the re-scaling ratio is $R = 800$, so that the frequency of the input signal satisfies the small-parameter requirement of SR. The changing trends of the output SNR of the three systems versus the input signal frequency are shown in Fig. 5, and each data point is obtained by an average of 100 independent experiments. Obviously, the output SNRs of the feedback MSR system and the CBSR

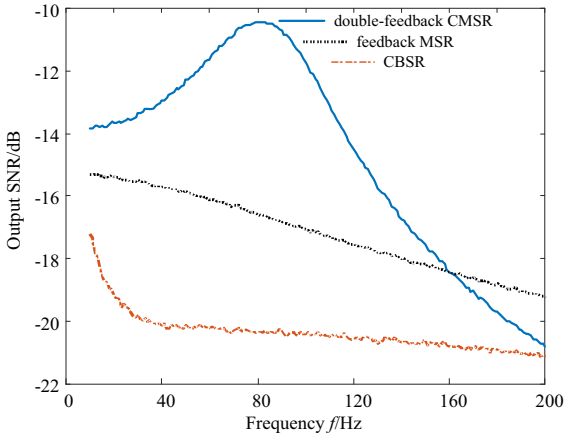

Fig. 5 System output frequency response curves ($a_1 = a_2 = 1$, $k_1 = -0.5$, $k_2 = 0.5$)

system monotonically decrease as the frequency of the input signal increases. This indicates that the two systems have better enhanced extraction capability for low-frequency signals, and the system output behavior exhibits low-pass filtering characteristics. Different from the two systems, the output SNR of the proposed system shows a trend of increasing first and then decreasing with the increase of the frequency of the input signal, indicating that the output of the proposed system presents band-pass filtering behavior. Therefore, from the perspective of signal processing, the system proposed in this paper can be regarded as a band-pass filter, which can suppress low-frequency and high-frequency noise interferences while strengthening the target signal. Considering that the signals in engineering practice are mostly large-parameter signals, compared with the above two systems, the proposed system is more conducive to achieve enhanced extraction of target signals and improve the detection performance of weak signals.

It can be found from the above analysis that by adding double feedback to the cascaded monostable system, the proposed system can not only generate SR phenomenon, but also exhibit band-pass filtering characteristics different from the CBSR system. This indicates that feedback control plays an important role in changing the system performance. In the following, a set of numerical experiments are carried out to further analyze the influence of the feedback coefficients on the system output frequency response. On the premise that the system parameters a_1 and a_2 are both 1, Fig. 6 illustrates the changing trends of the system output SNR versus the input signal frequency under different feedback coefficients k_1 and k_2. In Fig. 6a, when the feedback coefficient k_1 is around 0, the proposed system presents a low-pass filtering effect, but as the feedback coefficient k_1 gradually decreases, the system output SNR increases first and then decreases versus the input signal frequency, indicating that the proposed system has the effect of band-pass filtering. When the feedback coefficient is $k_2 = -0.5$, the influence of the feedback coefficient k_1 on the frequency response of the system output is shown in Fig. 6b. Comparing Fig. 6a with Fig. 6b, the two have similar trends in the system output SNR, but the effect in Fig. 6a is more noticeable. Therefore, when the feedback coefficient k_1 is less than zero, the proposed system presents band-pass filtering behavior. Figure 6c, d displays the influence of the feedback coefficient k_2 on the frequency response of the proposed system output when the feedback coefficients $k_1 = 0.5$ and $k_1 = -0.5$, respectively. As shown in Fig. 6c, with the decrease of the feedback coefficient k_2, the system output SNR decreases monotonically with the increase of the frequency of input signal, indicating that the proposed system exhibits low-pass filtering behavior, which is suitable for the detection of low-frequency input signals. In Fig. 6d, when the feedback coefficient k_2 is approximately between 0 and 1.5, the system output SNR increases first and then decreases with the increase of the frequency of input signal, indicating that the proposed system has band-pass filtering effect. However, when the feedback coefficient k_2 is less than zero, the system output SNR decreases monotonically, and the proposed system has been converted into a low-pass filter. Therefore, through the above analysis, it can be concluded that when the feedback coefficient k_1 is greater than zero, the proposed system has low-pass filtering characteristics regardless of the feedback coefficient k_2. When the feedback coefficient k_1 is less than zero and the feedback coefficient k_2 is greater than zero, the proposed system has band-pass filter characteristics. When the feedback systems k_1 and k_2 are both less than zero, the output behavior of the proposed system may present low-pass filtering effect, or band-pass filter effect. Accordingly, the feedback coefficients k_1 and k_2 have important influence on the frequency response characteristics of the system output. By selecting the appropriate combination of feedback coefficients, the desired system output

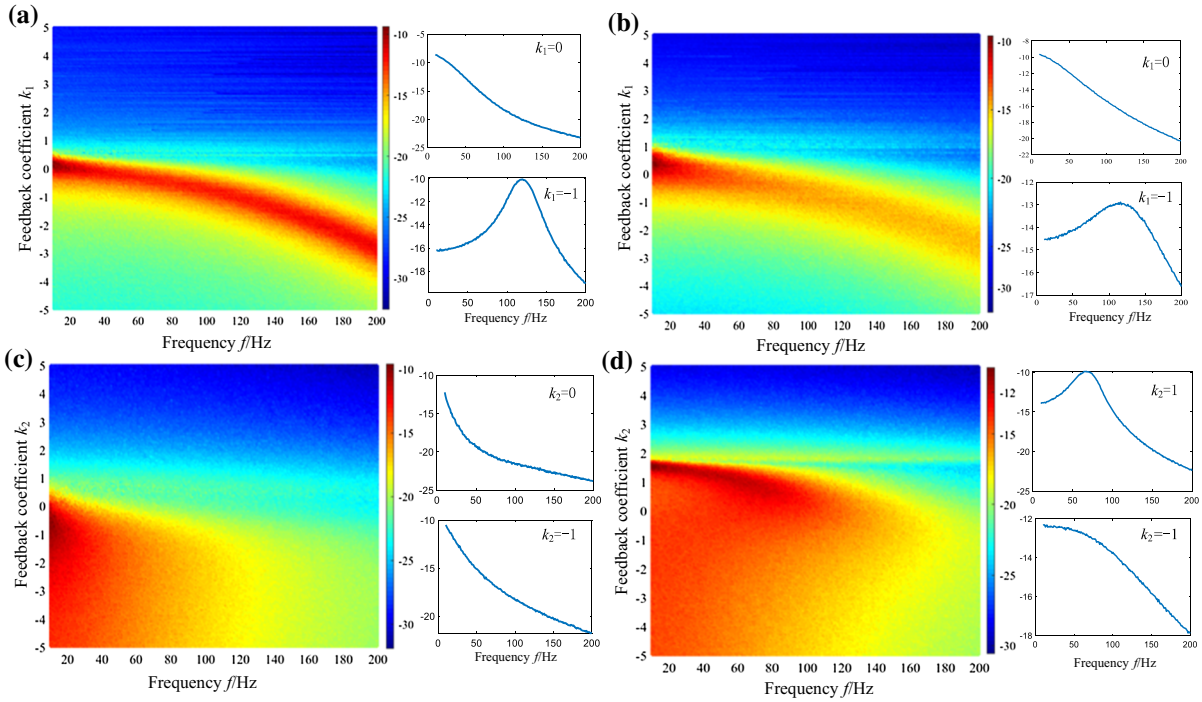

Fig. 6 Effects of different feedback coefficients on system output frequency responses: **a** k_2 = 0.5; **b** k_2 = -0.5; **c** k_1 = 0.5; **d** k_1 = -0.5

frequency response characteristics can be obtained to achieve enhanced extraction of weak signal features.

3 Numerical simulation

To verify the detection performance of the proposed double-feedback CMSR system for weak periodic signals, a simulated noisy signal is adopted and processed in this subsection. The simulated signal is $s(t) = 0.1\sin(2\pi f_0 t) + n(t)$ with the frequency f_0 = 20 Hz, the sampling frequency f_s = 5000 Hz, and the intensity of the added Gaussian white noise $\xi(t)$ is D = 1. The SNR of the signal $s(t)$ is − 28.97 dB. The time-domain waveform of the simulated signal and its spectrum are displayed in Fig. 7. It is observed that the time-domain waveform is disorderly, and the periodic signal is completely submerged in heavy noise. In the spectrum, the frequency components are abundant, and it is difficult to identify the frequency information of periodic signal due to the influence of background noise.

In order to detect the weak periodic signal and extract the frequency information, the proposed double-feedback CMSR system is employed to analyze the noisy signal $s(t)$. Meanwhile, the particle swarm optimization (PSO) algorithm is adopted to select the system parameters adaptively, and the optimal system parameter combination can be obtained by maximizing the system output SNR. Firstly, the searching

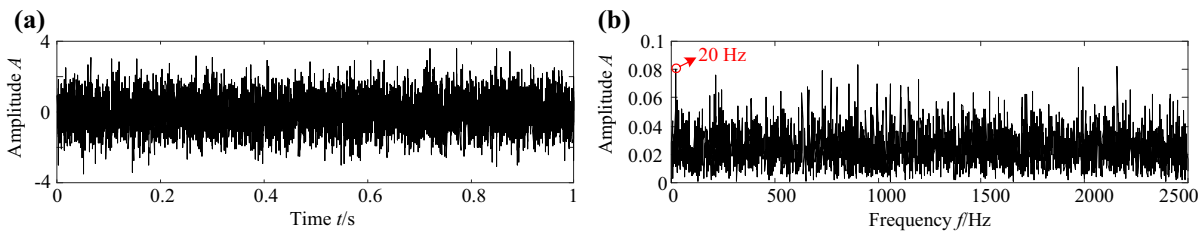

Fig. 7 Simulated signal $s(t)$: **a** the time-domain waveform; **b** the spectrum

ranges of parameters a_1 and a_2 are both [0.1 10], the searching ranges of the feedback coefficients k_1 and k_2 are both [-5 5], and the searching range of the re-scaling ratio R is [10 400]. The optimal detection results obtained are shown in Fig. 8a, b, and it can be seen that compared with the original signal shown in Fig. 7a, the oscillation period of the system output waveform is very obvious, and the noise reduces significantly. Moreover, it is worth noting that in the spectrum shown in Fig. 8b, the spectral peak at 20 Hz is very prominent, and the low-frequency interferences and high-frequency noise are suppressed effectively. This further verifies that when the feedback coefficients are $k_1 < 0$ and $k_2 > 0$, the proposed SR system has band-pass filtering performance.

Next, the searching range of feedback coefficient k_1 is adjusted to [0 5], and the searching ranges of other parameters remain unchanged, and the optimal detection results obtained are shown in Fig. 8c, d. It is observed that when the feedback coefficient is $k_1 > 0$, the proposed SR system can also detect the periodic signal with the frequency of 20 Hz, but the system output exhibits a low-pass filtering behavior. Although compared with the original signal, the noise in the system output waveform is significantly reduced, and the oscillation period is relatively obvious, the effect is far inferior to that in Fig. 8a, b. It still contains some low-frequency interferences, which is not conducive to the effective identification of the target signal features. The above analysis indicates that the performance of the proposed SR system is closely related to the feedback coefficients, and different parameter combinations enable the system to exhibit different filtering characteristics. This is consistent with the previous analysis. Moreover, the SR system with band-pass filtering

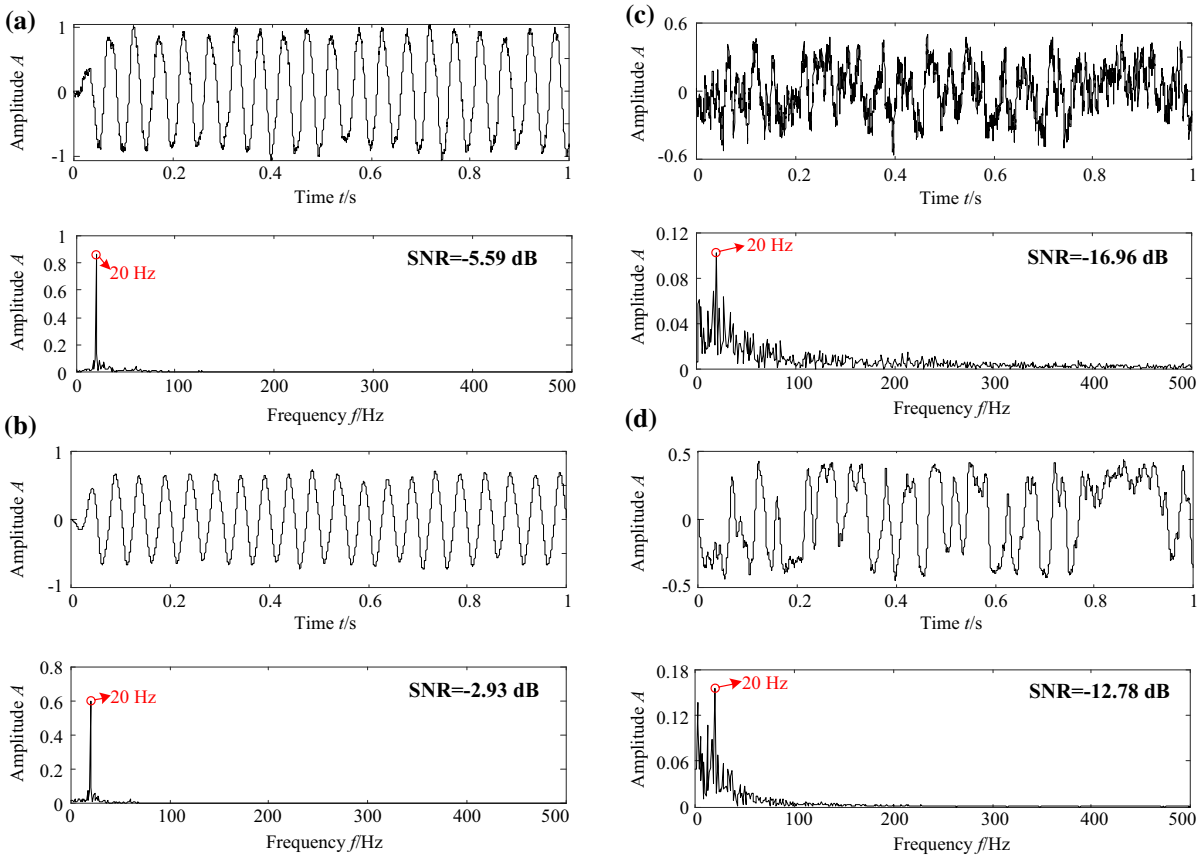

Fig. 8 Processing results of the proposed SR system with different parameters: **a** the first-stage output waveform and its spectrum, and **b** the second-stage output waveform and its spectrum (a_1 = 1.09, a_2 = 1.54, k_1 = -1.95, k_2 = 1.15, R = 102); **c** the first-stage output waveform and its spectrum, and **d** the second-stage output waveform and its spectrum (a_1 = 6.86, a_2 = 6.59, k_1 = 0.01, k_2 = 0.26, R = 286)

performance has a strong ability for extracting features of weak periodic signals.

Furthermore, by comparing the output waveforms of the two subsystems (Fig. 8a–d), the output waveform of the second-stage subsystem is smoother and the high-frequency dithering is smaller, whether it is a low-pass filtering output or a band-pass filtering output. This indicates that both subsystems in the proposed system generate resonance phenomenon, and connecting systems in series helps to smooth the system output further and improve the system output SNR. For comparison, the feedback MSR system, the CBSR system and the UBSR system are also applied to process the simulated signal $s(t)$. Similarly, the PSO algorithm is used to adaptively select the system parameters, and the optimal detection results obtained are displayed in Fig. 9. Firstly, it can be seen from Fig. 9a, b that although the feedback MSR system and CBSR system can detect the target signal with the frequency of 20 Hz, the time-domain waveforms are still disorderly and contain many low-frequency interferences, which affects the efficient identification of target signal features. This is consistent with the previous analysis; that is, the two SR systems perform low-pass filtering on the input signal, which cannot effectively suppress the influence of the low-frequency interferences on the target signal. Secondly, it is observed from Fig. 9c that the output of the UBSR system presents band-passing filtering behavior, and the oscillation period of the output waveform is more obvious than that in Fig. 9a, b, but it is far worse than that in Fig. 8b. Moreover, in addition to the target signal frequency component of 20 Hz, there are some interference components in the spectrum, and the

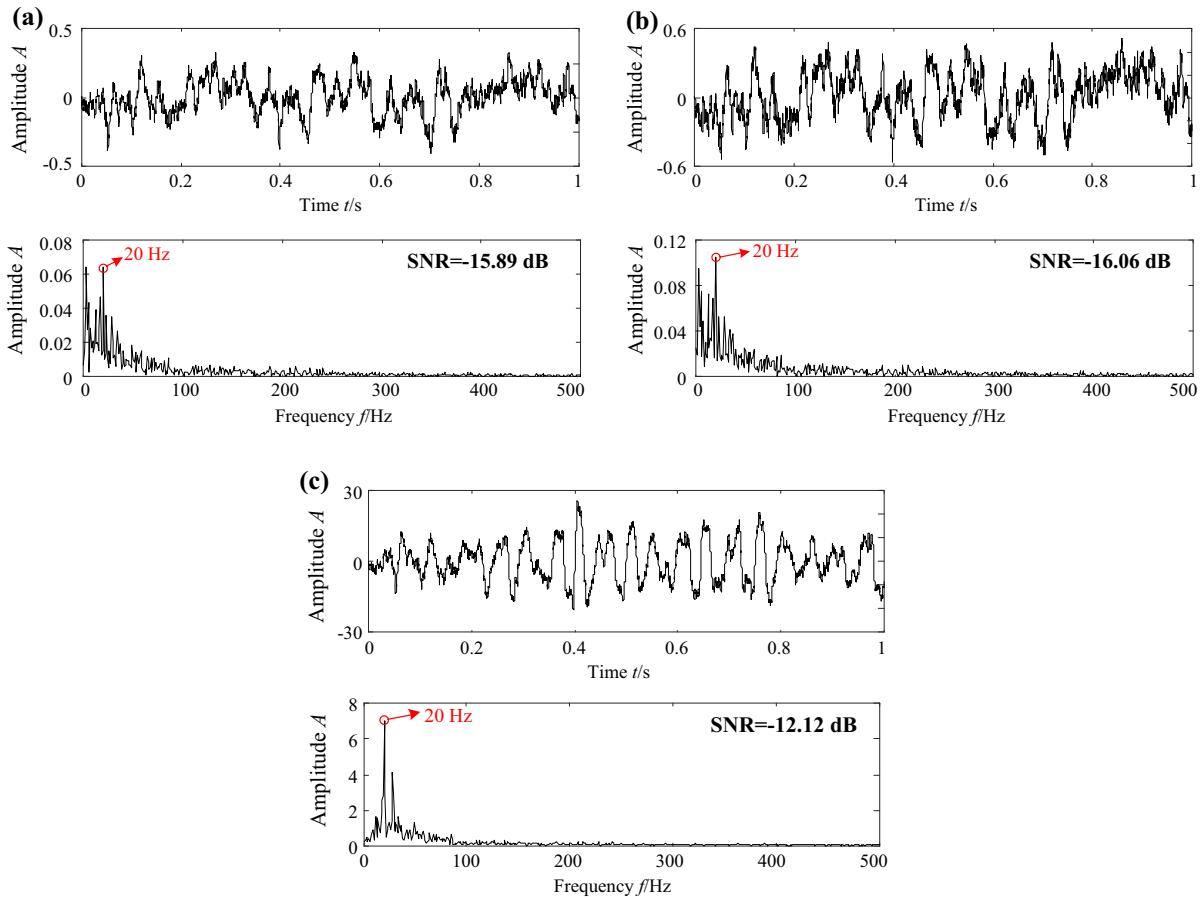

Fig. 9 Comparison results: **a** the output waveform and spectrum of feedback MSR system (a = 3.21, k = -0.49, R = 117); **b** the output waveform and spectrum of CBSR system (a = 3.18, b = 5.99, R = 209); **c** the output waveform and spectrum of UBSR system (a = 1.66, b = 3.74, γ = 1.6, R = 28)

system output SNR is much lower than the SR system proposed in this paper. Therefore, the above analysis demonstrates that the proposed system not only can generate resonance phenomenon, but also outperforms other SR systems in weak signal detection, which can be used for the features extraction of weak periodic signals.

4 Practical application

In the vibration monitoring of rotating machinery, when some key components such as gears and bearings fail, not only the collected vibration signals contain a large amount of noise interferences, but also the characteristic frequencies related to the faults in signals are mostly tens to hundreds of Hz. Therefore, when using the SR to analyze the vibration signals of the mechanical system for extracting the periodic component features, compared with the CBSR system with low-pass filtering characteristics, the SR system with band-pass filtering performance can not only enhance the target signal features by using the high-frequency noise energy, but also suppress the low-frequency interferences to further highlight the target signal. This is more suitable for the extraction of weak signal features in the fault detection of rotating machinery. According to the vibration mechanism of rolling bearings, when a localized failure occurs in a rolling bearing, a series of periodic impulses are generated in vibration signals. The rate of generation of the impulses is called fault characteristic frequency of rolling bearing. In order to extract and identify the fault characteristic frequency of rolling bearing, we can perform the frequency analysis on the envelope of vibration signal obtained by amplitude demodulation [1]. Accordingly, a weak signal detection method based on the double-feedback CMSR system is proposed for fault feature extraction of rolling bearings. In the proposed method, the envelope of vibration signal obtained by Hilbert transform is input into the double-feedback CMSR system to extract and enhance the fault features of rolling bearings. In addition, to obtain the optimal combination of the system parameters, the PSO algorithm is employed to adaptively select and optimize the parameters a_1, a_2, k_1, k_2 and the re-scaling ratio R, and then the optimal detection results are obtained by maximizing the output SNR of the proposed system. In the following, two sets of rolling bearing vibration data are adopted to analyze the performance of the proposed method and validate the effectiveness and superiority of the proposed method by comparison with other SR methods.

4.1 Rolling bearing fault feature extraction of electric locomotive

The vibration data of rolling bearing were derived from the fault test platform for rolling bearings of electric locomotive. In the experiment, the type of tested bearing was 552732QT, the rotating speed was 602 r/min, and the vibration signal was collected by the acceleration sensor at a sampling rate of 12.8 kHz. Figure 10 shows the collected vibration signal and its spectra. It can be observed that there are some relatively obvious impulses in the time-domain waveform, but the frequency components are complex in the spectrum, and it is difficult to find valuable feature information related to the bearing failure. The original signal is demodulated by Hilbert transform, and the obtained envelope spectrum is displayed in Fig. 10c. It can be found that in addition to the prominent spectral peak at the rotating frequency f_r, an inconspicuous spectral peak at 98 Hz can be found, which is approximately identical to the inner ring fault characteristic frequency 98.17 Hz of rolling bearing. However, due to the influence of noise and interference components, the fault features of rolling bearing are weak and difficult to identify effectively.

In order to extract the fault features of rolling bearing from the vibration signal, the proposed method is used for further analysis. In the PSO algorithm, the searching ranges of system parameters a_1 and a_2 are [0.1 10], the searching ranges of the feedback coefficients k_1 and k_2 are both [-5 5], and the searching range of the re-scaling ratio R is [100 1000]. The detection results obtained are shown in Fig. 11, and the system output SNR is $-$ 8.75 dB. Obviously, after being processed by the method proposed in this paper, the oscillation period of the output waveform is very obvious, and some low-frequency interferences and high-frequency noise are significantly reduced, the fault characteristic frequency of the rolling bearing in the spectrum is very prominent, thereby improving the identification accuracy of the rolling bearing fault features. Figure 12 illustrates the rolling bearing with inner ring damage.

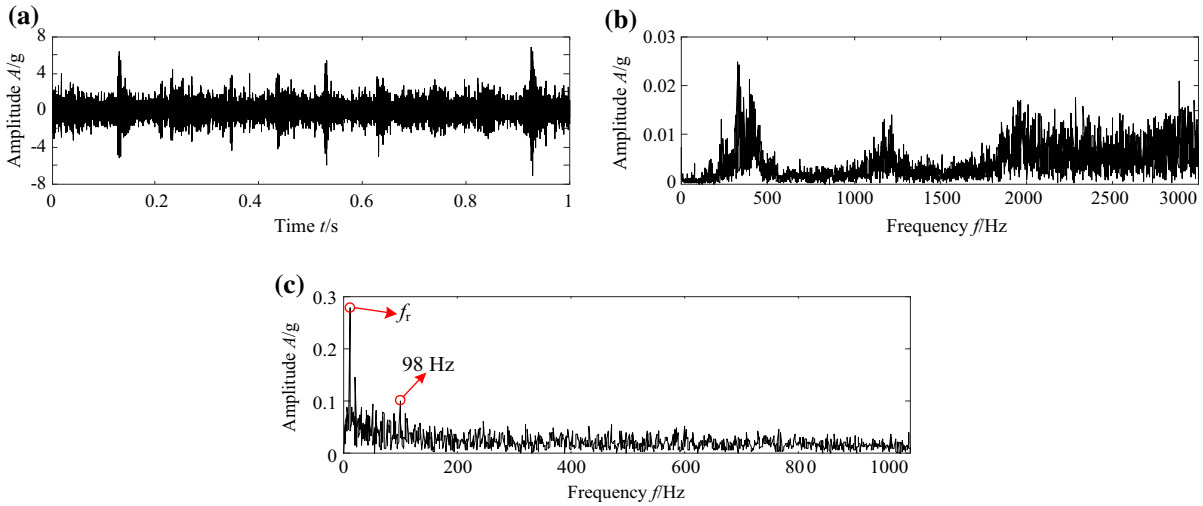

Fig. 10 Vibration signal of locomotive rolling bearing: **a** the time-domain waveform; **b** the spectrum; **c** the envelope spectrum

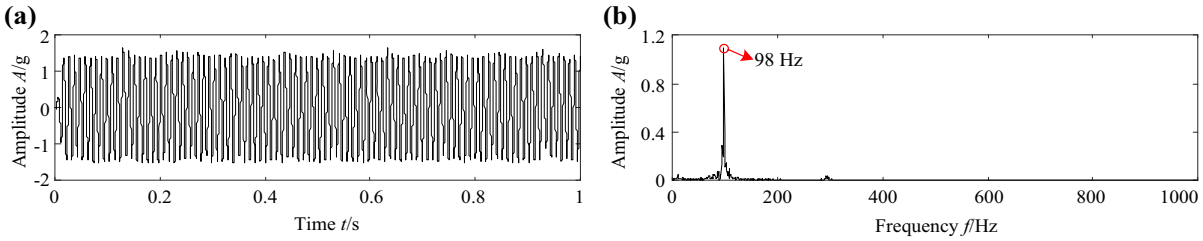

Fig. 11 Processing results of bearing vibration signal by the proposed method (a_1 = 0.11, a_2 = 0.69, k_1 = -4.66, k_2 = 1.74, R = 313): **a** the time-domain waveform; **b** the spectrum

Fig. 12 Inner ring abrasion of rolling bearing

In contrast, the CBSR system and the UBSR system are also applied to analyze the vibration signal of the rolling bearing. Moreover, in order to enable the CBSR system to better process large-parameter signals, the envelope of the original signal is first processed by high-pass filtering to remove some low-frequency interferences and then input to the CBSR system. The PSO algorithm is employed to adaptively select the parameters of CBSR system, the obtained detection results are shown in Fig. 13a, and the corresponding system parameters are a = 0.11, b = 9.18 and R = 283. The system output SNR is − 19.2 dB. It can be seen that due to some low-frequency interferences being filtered out in advance, a relatively obvious spectral peak appears at the fault characteristic frequency of the rolling bearing, but the output signal still contains much noise. Figure 13b displays the processing results of the UBSR system for the bearing vibration signal, and the corresponding system parameters a = 2.45, b = 0.24, γ = 1.34 and R = 172, the system output SNR is − 17.7 dB. Unlike the CBSR system, the UBSR system has band-pass filtering performance, which can suppress low-frequency interferences and high-frequency noise while enhancing the target signal. However, as shown in Fig. 13b, there are still many interferences near the frequency of

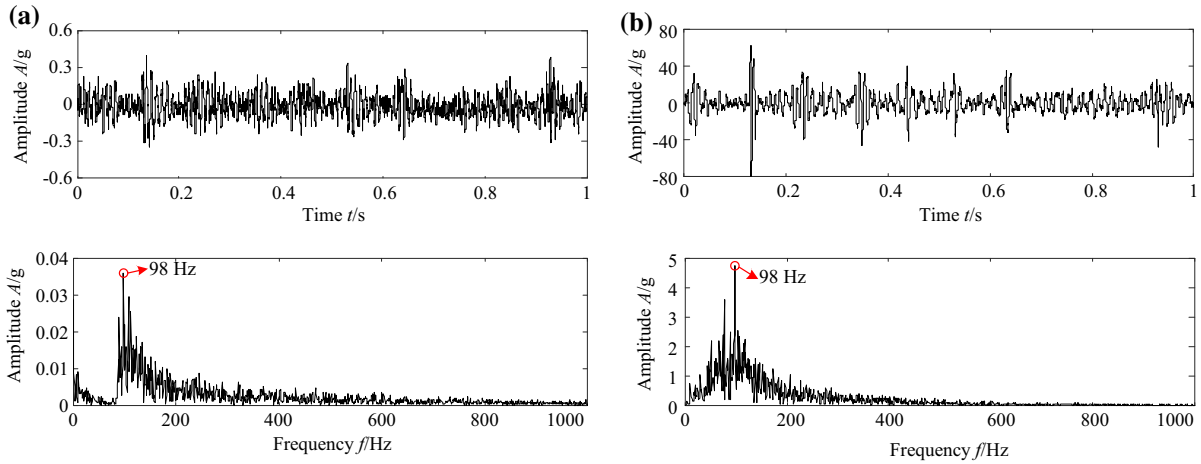

Fig. 13 **a** the output waveform and spectrum of the CBSR system; **b** the output waveform and spectrum of the UBSR system

target signal, and the feature extraction effect is inferior to that in Fig. 11. These results demonstrate that the proposed method has advantages in weak periodic signal detection as compared to the CBSR and UBSR methods.

4.2 Fault feature extraction of generator rolling bearing of wind turbine

In order to further verify the practicability and validity of the proposed method in the rolling bearing fault detection in engineering practice, the vibration data collected from the generator rolling bearing of an actual wind turbine in a wind farm were adopted for analysis. The acceleration sensor was used to acquire vibration signals of the generator bearing, and the installation position of the sensor in the field testing is shown in Fig. 14. The type of generator bearing was 6332M_FAG, and the rotating speed of generator was 1200 r/min. The sampling frequency was 12.8 kHz, and the data length was 12,800 points. Figure 15 shows the acquired vibration signal waveform and its spectra. Obviously, in the time-domain waveform and spectrum, except for the rotating frequency of 20 Hz, it is difficult to find valuable information relevant to the rolling bearing faults. After envelope extraction, in the envelope spectrum shown in Fig. 15c, apart from the rotating frequency, a relatively obvious spectral peak can be found at 109 Hz. By calculating the fault characteristic frequencies of the rolling bearing, it can be found that the spectral peak of 109 Hz is approximately consistent with the fault characteristic frequency 108.3 Hz of the bearing inner ring. However, due to the influence of strong background noise, the fault features are submerged and are not easily identified.

In order to further extract the fault features of generator bearing, the proposed method is adopted to analyze the vibration signal of generator bearing. The optimal detection results obtained are shown in

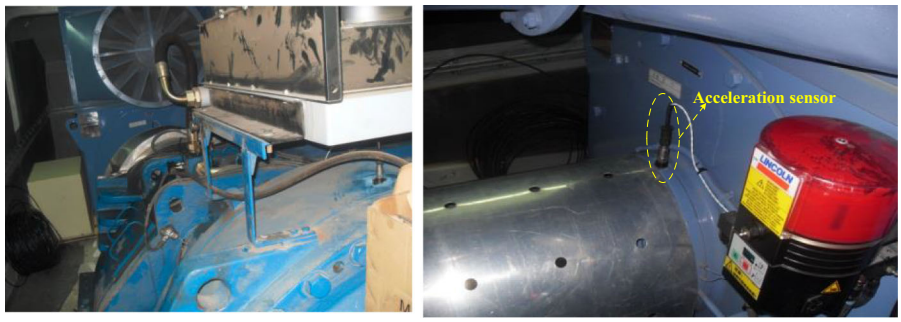

Fig. 14 Field vibration testing of Wind turbine and the installation location of vibration sensor of generator

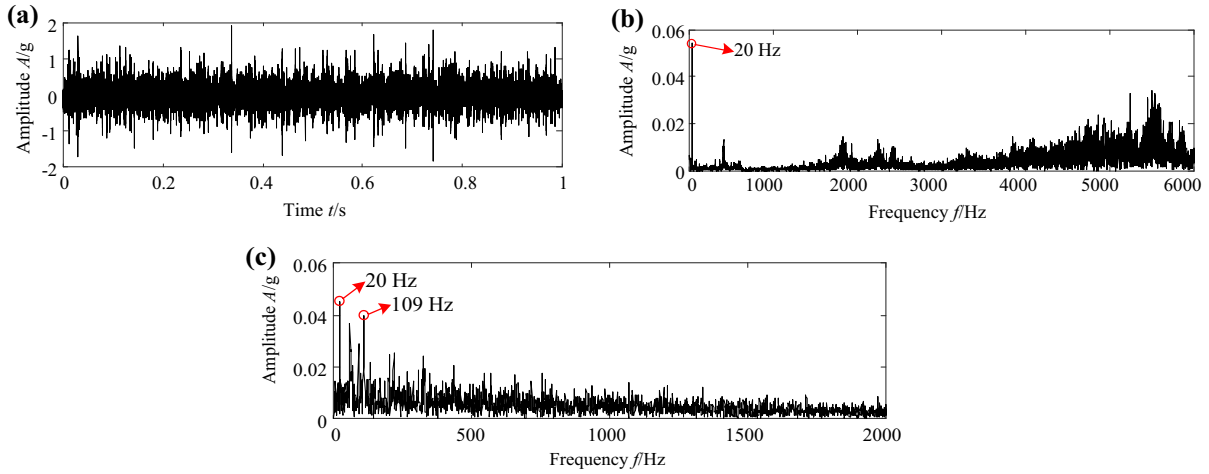

Fig. 15 Generator bearing vibration signal: **a** the time-domain waveform; **b** the spectrum; **c** the envelope spectrum

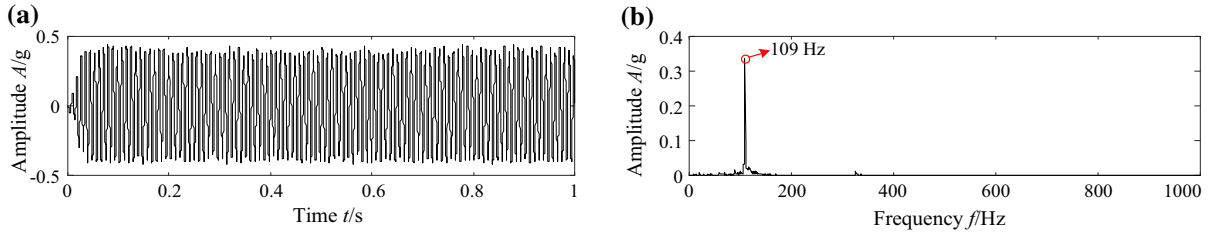

Fig. 16 Processing results of generator bearing vibration signal by the proposed method: **a** the time-domain waveform; **b** the spectrum

Fig. 16, and the corresponding parameters are $a_1 = 0.7$, $a_2 = 7.83$, $k_1 = -4.96$, $k_2 = 1.24$ and $R = 322$, and the system output SNR is -5.95 dB. Under such a combination of feedback coefficients, the proposed SR system presents band-pass filtering behavior. As shown in Fig. 16, in the spectrum, except for the noticeable spectral peak at the fault characteristic frequency of the rolling bearing, the remaining frequency components are effectively suppressed. According to the fault mechanism of rolling bearing [1], the above analysis results demonstrate that a localized damage may occur on the inner ring of generator bearing, and it is necessary to pay more attention to its operating status and detect regularly.

Similarly, Fig. 17 displays the processing results of the CBSR system and the UBSR system for the generator bearing vibration signal. For the results obtained by the CBSR system shown in Fig. 17a, the corresponding system parameters are $a = 0.14$, $b = 6.51$ and $R = 859$, the system output SNR is -17.95 dB. In Fig. 17b, the parameters of UBSR system are $a = 1.27$, $b = 6.39$, $\gamma = 1.04$ and $R = 161$, and the system output SNR is -15.5 dB. Comparing Fig. 16 with Fig. 17, although the latter two methods can also extract the fault characteristic frequency of rolling bearing, the detection results still contain more or less interferences, and the feature extraction effect is inferior to that of the proposed method. Moreover, the CBSR system is susceptible to the low-frequency components, and it is necessary to filter out some low-frequency interferences before extracting relative high-frequency target signals. Therefore, through the above analysis, compared with the CBSR system and UBSR system, the proposed method has good performance in weak periodic signal detection and can be used for the fault feature extraction of rolling bearing.

5 Conclusion

In this paper, a double-feedback CBSR system was proposed, which was constructed by using two series-connected symmetric quartic monostable systems and

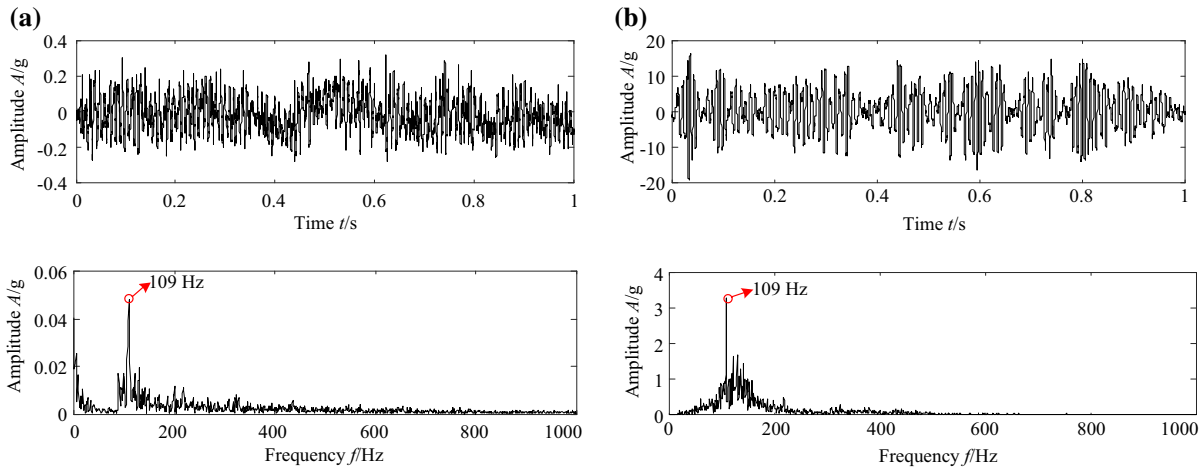

Fig. 17 **a** the output waveform and spectrum of the CBSR system; **b** the output waveform and spectrum of the UBSR system

two feedback coefficients. Taking the output SNR as the measurement index, the SR phenomenon of the proposed system driven by a weak periodic signal and Gaussian white noise was studied, and the influence of system parameters on the output performance of the system was analyzed. The following conclusions were drawn: (1) by introducing feedback control and serial structure, not only the response characteristics of the monostable system were altered, but also the system performance was improved, making the system output waveform smoother and the output SNR larger. (2) Compared with the model parameters a_1 and a_2, the feedback coefficients k_1 and k_2 have larger effect on the performance of the proposed system and with the different combinations of feedback coefficients, the proposed system output will exhibit a low-pass filtering or band-pass filtering behavior. (3) The performance of the proposed SR system outperformed the CBSR system and UBSR system in weak signal detection and can be used for the fault feature extraction of rolling bearings. The role of feedback control and multi-system synergy in a SR system was analyzed and verified in the paper, which can provide references for subsequent system control research and SR enhancement methods research.

In addition, this paper only considers the influence of feedback coefficients on the system performance and not consider the effect of time-delayed parameters. In fact, different time-delayed parameters can introduce different historical information. Therefore, the next research focus is to analyze the influence of different time-delayed parameters on the system performance, as well as the dependency of time-delayed parameters and feedback intensity, and then improve the performance through comprehensive consideration of multiple parameters. Moreover, the SNR is selected as the measurement index to guide the selection of algorithm parameters in the paper. If the target signal frequency is unknown, it is necessary to select other indexes or construct new indexes to improve the practicability of the proposed method in weak signal detection.

Acknowledgements This work was supported by the National Natural Science Foundation of China (Grant Nos. 51505415 and 61308065) and the Natural Science Foundation of Hebei Province (Grant Nos. E2017203142 and F2018203413). The authors would like to appreciate the anonymous reviewers for their valuable comments and suggestions.The authors declare that they have no conflict of interest.

References

1. Sawalhi, N., Randall, R.B., Endo, H.: The enhancement of fault detection and diagnosis in rolling element bearings using minimum entropy deconvolution combined with spectral kurtosis. Mech. Syst. Signal Process. **21**, 2616–2633 (2007)
2. Morales-Valdez, J., Alvarez-Icaza, L., Escobar, J.A.: Damage localization in a building structure during seismic excitation. Shock Vib. **2020**, 8859527 (2020)
3. Mohamad, T.H., Samadani, M., Natara, J.C.: Rolling element bearing diagnostics using extended phase space topology. J. Vib. Acoust. **140**(6), 061009 (2018)
4. Ghaderi, P., Amini, F.: Development of a new method for online parameter identification in seismically excited smart

building structures using virtual synchronization and adaptive control design. Appl. Math. Model **87**, 203–221 (2020)
5. Iatsenko, D., Mcclintock, P.V., Stefanovska, A.: Nonlinear mode decomposition: A noise-robust, adaptive decomposition method. Phys. Rev. E **92**(3–1), 032916 (2015)
6. Dragomiretskiy, K., Zosso, D.: Variational mode decomposition. IEEE Trans. Signal Process. **62**(3), 531–544 (2013)
7. Feng, Z.P., Lin, X.F., Zuo, M.J.: Joint amplitude and frequency demodulation analysis based on intrinsic time-scale decomposition for planetary gearbox fault diagnosis. Mech. Syst. Signal Process. **72–73**, 223–240 (2016)
8. Kedadouche, M., Thomas, M., Tahan, A.: A comparative study between empirical wavelet transforms and empirical mode decomposition methods: application to bearing defect diagnosis. Mech. Syst. Signal Process. **81**, 88–107 (2016)
9. Chen, X.W., Feng, Z.P.: Iterative generalized time-frequency reassignment for planetary gearbox fault diagnosis under nonstationary conditions. Mech. Syst. Signal Process. **80**, 429–444 (2016)
10. Blodt, M., Chabert, M., Regnier, J., Faucher, J.: Mechanical load fault detection in induction motors by stator current time-frequency analysis. IEEE Trans. Ind. Appl. **42**(6), 1454–1463 (2006)
11. Benzi, R., Sutera, A., Vulpiani, A.: The mechanism of stochastic resonance. J. Phys. Math. General. **14**(11), L453 (1981)
12. Lu, S.L., He, Q.B., Wang, J.: A review of stochastic resonance in rotating machine fault detection. Mech. Syst. Signal Process. **116**, 230–260 (2019)
13. He, Q.B., Wang, J., Liu, Y.B., Dai, D.Y., Kong, F.R.: Multiscale noise tuning of stochastic resonance for enhanced fault diagnosis in rotating machines. Mech. Syst. Signal Process. **28**, 443–457 (2012)
14. Mba, C.U., Makis, V., Marchesiello, S., Fasana, A., Garibaldi, L.: Condition monitoring and state classification of gearboxes using stochastic resonance and hidden Markov models. Measurement **126**, 76–95 (2018)
15. Liu, J.J., Leng, Y.G., Lai, Z.H., Fan, S.B.: Multi-frequency signal detection based on frequency exchange and re-scaling stochastic resonance and its application to weak fault diagnosis. Sensors **18**(5), 1325 (2018)
16. Lu, L., Yuan, Y., Wang, H., Zhao, X., Zheng, J.J.: A new second-order tristable stochastic resonance method for fault diagnosis. Symmetry Basel **11**(8), 965 (2019)
17. Li, Z.X., Shi, B.Q., Ren, X.P., Zhu, W.Y.: Research and application of weak fault diagnosis method based on asymmetric potential stochastic resonance. Meas Control UK **52**(5–6), 625–633 (2019)
18. He, C.B., Li, H.K., Li, Z.X., Zhao, X.W.: An improved bistable stochastic resonance and its application on weak fault characteristic identification of centrifugal compressor blades. J. Sound Vib. **442**, 677–697 (2019)
19. Qiao, Z.J., Lei, Y.G., Li, N.: Applications of stochastic resonance to machinery fault detection: a review and tutorial. Mech. Syst. Signal Process. **122**, 502–536 (2019)
20. McInnes, C.R., Gorman, D.G., Cartmell, M.P.: Enhanced vibrational energy harvesting using nonlinear stochastic resonance. J. Sound Vib. **318**(4–5), 655–662 (2008)
21. Yang, J.H., Sanjuan, M.A.F., Liu, H.G., Zhu, H.: Noise-induced resonance at the subharmonic frequency in bistable systems. Nonlinear Dyn. **87**(3), 1721–1730 (2017)
22. Qiao, Z.J., Lei, Y.G., Lin, J., Jia, F.: An adaptive unsaturated bistable stochastic resonance method and its application in mechanical fault diagnosis. Mech. Syst. Signal Process. **84**, 731–746 (2017)
23. Liu, H.G., Liu, X.L., Yang, J.H., Sanjuan, M.A.F., Cheng, G.: Detecting the weak high-frequency character signal by vibrational resonance in the duffing oscillator. Nonlinear Dyn. **89**(4), 2621–2628 (2017)
24. Zhang, G., Song, Y., Zhang, T.Q.: Stochastic resonance in a single-well system with exponential potential driven by levy noise. Chin. J. Phys. **55**(1), 85–95 (2017)
25. Agudov, N.V., Krichigin, A.V., Valenti, D., Spagnolo, B.: Stochastic resonance in a trapping overdamped monostable system. Phys. Rev. E **81**(5), 051123 (2010)
26. Yao, M.L., Xu, W., Ning, L.J.: Stochastic resonance in a bias monostable system driven by a periodic rectangular signal and uncorrelated noises. Nonlinear Dyn. **67**(1), 329–333 (2012)
27. Han, D.Y., Li, P., An, S.J., Shi, P.M.: Multi-frequency weak signal detection based on wavelet transform and parameter compensation band-pass multi-stable stochastic resonance. Mech. Syst. Signal Process. **70**, 995–1010 (2016)
28. Lai, Z.H., Liu, J.S., Zhang, H.T., Zhang, C.L., Zhang, J.W., Duan, D.Z.: Multi-parameter-adjusting stochastic resonance in a standard tri-stable system and its application in incipient fault diagnosis. Nonlinear Dyn. **96**(3), 2069–2085 (2019)
29. Lei, Y.G., Qiao, Z.J., Xu, X.F., Lin, J., Niu, S.T.: An underdamped stochastic resonance method with stable-state matching for incipient fault diagnosis of rolling element bearings. Mech. Syst. Signal Process. **94**, 148–164 (2017)
30. Li, J.M., Li, M., Zhang, J.F.: Rolling bearing fault diagnosis based on time-delayed feedback monostable stochastic resonance and adaptive minimum entropy deconvolution. J. Sound Vib. **401**, 139–151 (2017)
31. Tsimring, L.S., Pikovsky, A.: Noise-induced dynamics in bistable systems with delay. Phys. Rev. Lett. **87**(25), 250602 (2001)
32. Hu, B.B., Li, B.: Fault diagnosis of gearbox using multi-time-delayed feedback stochastic resonance. Proc. Inst. Mech. Eng. Part C J. Mech. **231**(19), 3541–3552 (2017)
33. Lu, S.L., He, Q.B., Zhang, H.B., Kong, F.R.: Enhanced rotating machine fault diagnosis based on time-delayed feedback stochastic resonance. J. Vib. Acoust. **137**(5), 051008 (2015)
34. He, H.L., Wang, T.Y., Leng, Y.G., Zhang, Y., Li, Q.: Study on non-linear filter characteristic and engineering application of cascaded bistable stochastic resonance system. Mech. Syst. Signal Process. **21**(7), 2740–2749 (2007)
35. Guo, W., Zhou, Z.M., Chen, C., Li, X.: Multi-frequency weak signal detection based on multi-segment cascaded stochastic resonance for rolling bearings. Microelectron. Reliab. **75**, 239–252 (2017)
36. Zhao, R., Yan, R.Q., Gao, R.X.: Dual-scale cascaded adaptive stochastic resonance for rotary machine health monitoring. J. Manuf. Syst. **32**(4), 529–535 (2013)

37. Duan, F.B., Chapeau-Blondeau, F., Abbott, D.: Stochastic resonance in a parallel array of nonlinear dynamical elements. Phys. Lett. A **372**(13), 2159–2166 (2008)
38. Liu, J., Wang, Y.G., Zhai, Q.Q., Liu, J.: Parameter allocation of parallel array bistable stochastic resonance and its application in communication systems. Chin. Phys. B **25**(10), 100501 (2016)
39. Kenfack, A., Singh, K.P.: Stochastic resonance in coupled underdamped bistable systems. Phys. Rev. E **82**(4), 046224 (2010)
40. He, M.J., Xu, W., Sun, Z.K., Jia, W.T.: Characterizing stochastic resonance in coupled bistable system with poisson white noises via statistical complexity measures. Nonlinear Dyn. **88**(2), 1163–1171 (2017)
41. Nicolis, C., Nicolis, G.: Coupling-enhanced stochastic resonance. Phys. Rev. E **96**(4), 042214 (2017)